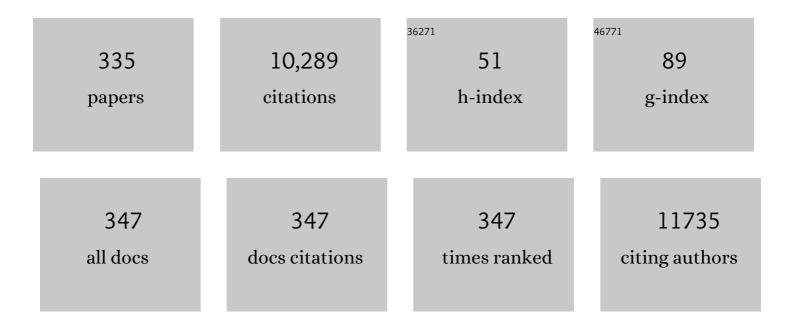
Carsten Ronning

List of Publications by Year in descending order

Source: https://exaly.com/author-pdf/8457916/publications.pdf Version: 2024-02-01



#	Article	IF	CITATIONS
1	The disappearance and return of nanoparticles upon low energy ion irradiation. Nanotechnology, 2022, 33, 035703.	1.3	5
2	Applications of Hybrid Metalâ€Dielectric Nanostructures: State of the Art. Advanced Photonics Research, 2022, 3, .	1.7	30
3	Laser energy absorption and x-ray generation in nanowire arrays irradiated by relativistically intense ultra-high contrast femtosecond laser pulses. Physics of Plasmas, 2022, 29, .	0.7	9
4	Low optical losses in plasmonic TiN thin films implanted with silver and gold. Optical Materials, 2022, 123, 111936.	1.7	4
5	Wideâ€Bandgap Double Perovskites with Multiple Longitudinalâ€Optical Phonon Scattering. Advanced Functional Materials, 2022, 32, .	7.8	20
6	Defect induced stress in ion irradiated nanocrystalline Ge2Sb2Te5. Materials Letters, 2022, , 132249.	1.3	0
7	Fe implantation induced lattice defects and their recovery in GaN. Hyperfine Interactions, 2022, 243, 1.	0.2	0
8	Tuning nanowire lasers <i>via</i> hybridization with two-dimensional materials. Nanoscale, 2022, 14, 6822-6829.	2.8	2
9	A photonic integrated circuit–based erbium-doped amplifier. Science, 2022, 376, 1309-1313.	6.0	95
10	Tuning carrier density and phase transitions in oxide semiconductors using focused ion beams. Nanophotonics, 2022, 11, 3923-3932.	2.9	10
11	Tunable Infrared Optics Enabled by Defect-Engineering of Vanadium Dioxide Using Focused Ion Beam. , 2021, , .		0
12	Luminescence of ZnO nanocrystals in silica synthesized by dual (Zn, O) implantation and thermal annealing. Journal Physics D: Applied Physics, 2021, 54, 265104.	1.3	9
13	Ellipticity dependent excitation and high harmonic generation from intense mid-IR laser pulses in ZnO. , 2021, , .		0
14	Contribution of free carriers to light absorption upon intense light-semiconductor interaction. , 2021, , .		0
15	Coupling of a single tin-vacancy center to a photonic crystal cavity in diamond. Applied Physics Letters, 2021, 118, .	1.5	35
16	Role of free-carrier interaction in strong-field excitations in semiconductors. Physical Review B, 2021, 104, .	1.1	1
17	Fast recovery of ion-irradiation-induced defects in Ge ₂ Sb ₂ Te ₅ thin films at room temperature. Optical Materials Express, 2021, 11, 3535.	1.6	2
18	Polarization Dependent Excitation and High Harmonic Generation from Intense Mid-IR Laser Pulses in ZnO. Nanomaterials, 2021, 11, 4.	1.9	9

#	Article	IF	CITATIONS
19	Tuning exciton recombination rates in doped transition metal dichalcogenides. Optical Materials: X, 2021, 12, 100097.	0.3	5
20	Engineering Optical Materials Using Focused Ion Beams. , 2021, , .		0
21	Polarization dependent multiphoton absorption in ZnO thin films. Journal Physics D: Applied Physics, 2020, 53, 055102.	1.3	6
22	Determination of the full deformation tensor by multi-Bragg fast scanning nano X-ray diffraction. Journal of Applied Crystallography, 2020, 53, 99-106.	1.9	2
23	Photoluminescence of ZnO/ZnMgO heterostructure nanobelts grown by MBE. Nanotechnology, 2020, 31, 135604.	1.3	11
24	On the Germanium Incorporation in Cu ₂ ZnSnSe ₄ Kesterite Solar Cells Boosting Their Efficiency. ACS Applied Energy Materials, 2020, 3, 558-564.	2.5	11
25	Microwave AC Resonance Induced Phase Change in Sb ₂ Te ₃ Nanowires. Nano Letters, 2020, 20, 8668-8674.	4.5	1
26	Hot electrons in a nanowire hard X-ray detector. Nature Communications, 2020, 11, 4729.	5.8	4
27	Interplay of Performanceâ€Limiting Nanoscale Features in Cu 2 ZnSn(S,Se) 4 Solar Cells. Physica Status Solidi (A) Applications and Materials Science, 2020, 217, 2000456.	0.8	3
28	In-Operando Nanoscale X-ray Analysis Revealing the Local Electrical Properties of Rubidium-Enriched Grain Boundaries in Cu(In,Ga)Se ₂ Solar Cells. ACS Applied Materials & Interfaces, 2020, 12, 57117-57123.	4.0	7
29	Conversionless efficient and broadband laser light diffusers for high brightness illumination applications. Nature Communications, 2020, 11, 1437.	5.8	52
30	Revealing the origin of the beneficial effect of cesium in highly efficient Cu(In,Ga)Se2 solar cells. Nano Energy, 2020, 71, 104622.	8.2	25
31	Evaluation of carrier density and mobility in Mn ion-implanted GaAs:Zn nanowires by Raman spectroscopy. Nanotechnology, 2020, 31, 205705.	1.3	2
32	Grayscale Nanopatterning of Phase-Change Materials for Subwavelength-Scaled, Inherently Planar, Nonvolatile, and Reconfigurable Optical Devices. ACS Applied Nano Materials, 2020, 3, 4486-4493.	2.4	7
33	Thermal annealing of Ag implanted silicon: Relationship between structural and optical properties. Science of Sintering, 2020, 52, 207-217.	0.5	1
34	Toward Frequency-Selective Surfaces via Doping of Zinc Oxide with a Focused Ion Beam. , 2020, , .		0
35	Formation of Ag nanoparticles in Si (100) wafers by single and multiple low energy Ag ions implantation. Surface and Coatings Technology, 2019, 377, 124913.	2.2	6
36	On the Optical Properties of Thinâ€Film Vanadium Dioxide from the Visible to the Far Infrared. Annalen Der Physik, 2019, 531, 1900188.	0.9	135

#	Article	IF	CITATIONS
37	Comprehensive porosity determination of combustion-deposited SiOx thin films and correlation with FTIR signal. Surface and Coatings Technology, 2019, 375, 256-265.	2.2	1
38	Fe3C nanoparticle formation in Fe implanted HOPG and CVD diamond. Hyperfine Interactions, 2019, 240, 1.	0.2	0
39	Observation and manipulation of CICSe phase formation in a two stage sequential process. Applied Physics Letters, 2019, 115, 143901.	1.5	Ο
40	Silicon nanostructuring by Ag ions implantation through nanosphere lithography mask. Optical Materials, 2019, 88, 508-515.	1.7	6
41	Transition Metal and Rare Earth Element Doped Zinc Oxide Nanowires for Optoelectronics. Physica Status Solidi (B): Basic Research, 2019, 256, 1800604.	0.7	30
42	Strong Light-Field Driven Nanolasers. Nano Letters, 2019, 19, 3563-3568.	4.5	4
43	Dynamics and Interactions of Semiconductor Nanowires for Optoelectronics. Physica Status Solidi (B): Basic Research, 2019, 256, 1900127.	0.7	Ο
44	Raman characterization of single-crystalline Ga0.96Mn0.04As:Zn nanowires realized by ion-implantation. Nanotechnology, 2019, 30, 335202.	1.3	3
45	Single nanowire defined emission properties of ZnO nanowire arrays. Journal Physics D: Applied Physics, 2019, 52, 295101.	1.3	4
46	Controlling the p-type conductivity of SnO by doping with nitrogen and hydrogen. Journal of Applied Physics, 2019, 125, .	1.1	14
47	Culturing and patch clamping of Jurkat T cells and neurons on Al ₂ O ₃ coated nanowire arrays of altered morphology. RSC Advances, 2019, 9, 11194-11201.	1.7	9
48	Electroluminescence of intrashell transitions in Eu doped single ZnO nanowires. Nanotechnology, 2019, 30, 095201.	1.3	5
49	Improving gas sensing by CdTe decoration of individual Aerographite microtubes. Nanotechnology, 2019, 30, 065501.	1.3	8
50	Review on the dynamics of semiconductor nanowire lasers. Semiconductor Science and Technology, 2018, 33, 033001.	1.0	24
51	Flat Optical and Plasmonic Devices Using Areaâ€5elective Ionâ€Beam Doping of Silicon. Advanced Optical Materials, 2018, 6, 1701027.	3.6	12
52	Enhancement of the Sub-Band-Gap Photoconductivity in ZnO Nanowires through Surface Functionalization with Carbon Nanodots. Journal of Physical Chemistry C, 2018, 122, 1852-1859.	1.5	23
53	Embedded Optics: Flat Optical and Plasmonic Devices Using Area elective Ionâ€Beam Doping of Silicon (Advanced Optical Materials 5/2018). Advanced Optical Materials, 2018, 6, 1870019.	3.6	1
54	Monolithic Doped-Semiconductor Platform for Optical Devices in the Infrared. , 2018, , .		0

#	Article	IF	CITATIONS
55	Metasurfaces Enabled by Locally Tailoring Disorder in Phase-Change Materials. ACS Photonics, 2018, 5, 5103-5109.	3.2	12
56	Overall Distribution of Rubidium in Highly Efficient Cu(In,Ga)Se ₂ Solar Cells. ACS Applied Materials & Interfaces, 2018, 10, 40592-40598.	4.0	44
57	Magnetic nanocluster formation of Fe ions embedded in SiO2 and Al2O3 substrates. MRS Advances, 2018, 3, 2603-2608.	0.5	0
58	Hard X-ray Generation from ZnO Nanowire Targets in a Non-Relativistic Regime of Laser-Solid Interactions. Applied Sciences (Switzerland), 2018, 8, 1728.	1.3	10
59	Ion beam designed metasurfaces. , 2018, , .		0
60	Paramagnetic, NIR â€luminescent Nd 3+ ―and Gd 3+ â€doped fluorapatite as contrast agent for multimodal biomedical imaging. Journal of the American Ceramic Society, 2018, 101, 4441-4446.	1.9	2
61	Dynamics of nanoparticle morphology under low energy ion irradiation. Nanotechnology, 2018, 29, 314002.	1.3	7
62	Discrepancy between integral and local composition in off-stoichiometric Cu2ZnSnSe4 kesterites: A pitfall for classification. Applied Physics Letters, 2017, 110, .	1.5	19
63	Influence of Silver Film Quality on the Threshold of Plasmonic Nanowire Lasers. Advanced Optical Materials, 2017, 5, 1600856.	3.6	22
64	X-ray emission generated by laser-produced plasmas from dielectric nanostructured targets. AIP Conference Proceedings, 2017, , .	0.3	4
65	Excitation Energy Dependent Ultrafast Luminescence Behavior of CdS Nanostructures. ACS Photonics, 2017, 4, 1067-1075.	3.2	9
66	Local atomic environment of the Cu-related defect in zinc oxide. Journal Physics D: Applied Physics, 2017, 50, 145105.	1.3	1
67	Gate-controlled heat generation in ZnO nanowire FETs. Physical Chemistry Chemical Physics, 2017, 19, 14042-14047.	1.3	2
68	Sputtering and redeposition of ion irradiated Au nanoparticle arrays: direct comparison of simulations to experiments. New Journal of Physics, 2017, 19, 013023.	1.2	13
69	Ion Beam Induced Charge analysis of diamond diodes. Nuclear Instruments & Methods in Physics Research B, 2017, 404, 259-263.	0.6	3
70	Formation of superparamagnetic nanoclusters in Fe implanted Al2O3. Nuclear Instruments & Methods in Physics Research B, 2017, 409, 221-223.	0.6	0
71	Evolution of Metallicity in Vanadium Dioxide by Creation of Oxygen Vacancies. Physical Review Applied, 2017, 7, .	1.5	88
72	Growth of 18 O isotopicallyÂenriched ZnO nanorods by two novel VPT methods. Journal of Crystal Growth, 2017, 460, 85-93.	0.7	2

#	Article	IF	CITATIONS
73	Dynamical Tuning of Nanowire Lasing Spectra. Nano Letters, 2017, 17, 6637-6643.	4.5	19
74	Evolution of structural and optical properties of Ag implanted CrN thin films with annealing temperature. Journal of Alloys and Compounds, 2017, 729, 671-678.	2.8	6
75	Ion beam irradiation of nanostructures: sputtering, dopant incorporation, and dynamic annealing. Semiconductor Science and Technology, 2017, 32, 109401.	1.0	0
76	Epsilon-Near-Zero Substrate Engineering for Ultrathin-Film Perfect Absorbers. Physical Review Applied, 2017, 8, .	1.5	88
77	Clustering of gold particles in Au implanted CrN thin films: The effect on the SPR peak position. Applied Surface Science, 2017, 426, 667-673.	3.1	11
78	Low-loss and tunable near-zero-epsilon titanium nitride. Optical Materials, 2017, 72, 775-780.	1.7	14
79	In operando x-ray imaging of nanoscale devices: Composition, valence, and internal electrical fields. Science Advances, 2017, 3, eaao4044.	4.7	39
80	Rubidium segregation at random grain boundaries in Cu(In,Ga)Se2 absorbers. Nano Energy, 2017, 42, 307-313.	8.2	70
81	Flame based growth of ZnO nano- and microstructures for advanced optical, multifunctional devices, and biomedical applications (Conference Presentation). , 2017, , .		1
82	From three-photon to tunnel ionization pumped ZnO nanolasers. , 2017, , .		0
83	X-ray emission from nanostructured targets irradiated by a relativistically intense mid-infrared driver. , 2017, , .		0
84	High temperature limit of semiconductor nanowire lasers. Applied Physics Letters, 2017, 110, 173103.	1.5	12
85	Enhanced absorption and cavity effects of three-photon pumped ZnO nanowires. Applied Physics Letters, 2017, 111, 213106.	1.5	7
86	Carrier density driven lasing dynamics in ZnO nanowires. Nanotechnology, 2016, 27, 225702.	1.3	28
87	Compositional and electrical properties of line and planar defects in Cu(In,Ga)Se ₂ thin films for solar cells – a review. Physica Status Solidi - Rapid Research Letters, 2016, 10, 363-375.	1.2	47
88	CEMS study of defect annealing in Fe implanted AlN. Hyperfine Interactions, 2016, 237, 1.	0.2	1
89	High-level damage saturation below amorphisation in ion implanted β-Ga2O3. Nuclear Instruments & Methods in Physics Research B, 2016, 379, 85-90.	0.6	50
90	Synthesis, Morphological, and Electro-optical Characterizations of Metal/Semiconductor Nanowire Heterostructures. Nano Letters, 2016, 16, 3507-3513.	4.5	14

#	Article	IF	CITATIONS
91	Grain-boundary character distribution and correlations with electrical and optoelectronic properties of CuInSe2 thin films. Acta Materialia, 2016, 118, 244-252.	3.8	21
92	Shaping and compositional modification of zinc oxide nanowires under energetic manganese ion irradiation. Nanotechnology, 2016, 27, 175301.	1.3	12
93	Sensitivity of 57Fe emission Mössbauer spectroscopy to Ar and C induced defects in ZnO. Hyperfine Interactions, 2016, 237, 1.	0.2	2
94	Emission Mössbauer spectroscopy study of fluence dependence of paramagnetic relaxation in Mn/Fe implanted ZnO. Hyperfine Interactions, 2016, 237, 1.	0.2	1
95	Mode Switching and Filtering in Nanowire Lasers. Nano Letters, 2016, 16, 2878-2884.	4.5	25
96	Non-resonant Raman spectroscopy of individual ZnO nanowires via Au nanorod surface plasmons. Journal of Materials Chemistry C, 2016, 4, 1651-1657.	2.7	7
97	FAST/SPS sintering of nanocrystalline zinc oxide—Part I: Enhanced densification and formation of hydrogen-related defects in presence of adsorbed water. Journal of the European Ceramic Society, 2016, 36, 1207-1220.	2.8	56
98	Shape manipulation of ion irradiated Ag nanoparticles embedded in lithium niobate. Nanotechnology, 2016, 27, 145202.	1.3	30
99	Observation of Dielectrically Confined Excitons in Ultrathin GaN Nanowires up to Room Temperature. Nano Letters, 2016, 16, 973-980.	4.5	40
100	Active Optical Metasurfaces Based on Defect-Engineered Phase-Transition Materials. Nano Letters, 2016, 16, 1050-1055.	4.5	186
101	Low Energy Ion Beam Modification of Nanostructures. Springer Series in Surface Sciences, 2016, , 475-500.	0.3	4
102	Ultrafast ZnO nanowire lasers: nanoplasmonic acceleration of gain dynamics at the surface plasmon polariton frequency. , 2016, , .		0
103	Ultrafast plasmonic nanowire lasers near the surface plasmon frequency (Presentation Recording). Proceedings of SPIE, 2015, , .	0.8	1
104	Stoichiometry variation for the atomic layer deposition of SrxTiyOz from Sr(iPr3Cp)2, Ti[N(CH3)2]4 and H2O. Thin Solid Films, 2015, 577, 134-142.	0.8	4
105	Nature of AX Centers in Antimony-Doped Cadmium Telluride Nanobelts. Nano Letters, 2015, 15, 974-980.	4.5	10
106	Ion beam irradiation of nanostructures: sputtering, dopant incorporation, and dynamic annealing. Semiconductor Science and Technology, 2015, 30, 033001.	1.0	47
107	Nanocluster formation in Co/Fe implanted ZnO. Hyperfine Interactions, 2015, 230, 181-186.	0.2	2
108	Ultrafast Dynamics of Lasing Semiconductor Nanowires. Nano Letters, 2015, 15, 4637-4643.	4.5	51

#	Article	IF	CITATIONS
109	Adjusting the forming step for resistive switching in Nb2O5 by ion irradiation. Journal of Vacuum Science and Technology B:Nanotechnology and Microelectronics, 2015, 33, 01A105.	0.6	3
110	Anomalous Plastic Deformation and Sputtering of Ion Irradiated Silicon Nanowires. Nano Letters, 2015, 15, 3800-3807.	4.5	23
111	Dynamics of the phase formation process upon the low temperature selenization of Cu/In-multilayer stacks. Journal of Applied Physics, 2015, 117, 105302.	1.1	1
112	Improved Ga grading of sequentially produced Cu(In,Ga)Se2 solar cells studied by high resolution X-ray fluorescence. Applied Physics Letters, 2015, 106, .	1.5	20
113	Enhanced sputter yields of ion irradiated Au nano particles: energy and size dependence. Nanotechnology, 2015, 26, 325301.	1.3	22
114	ZnO/porous-Si and TiO2/porous-Si nanocomposite nanopillars. Journal of Vacuum Science and Technology A: Vacuum, Surfaces and Films, 2015, 33, 01A102.	0.9	6
115	Persistent Photoconductivity in ZnO Nanowires in Different Atmospheres. Advances in Condensed Matter Physics, 2014, 2014, 1-5.	0.4	27
116	Magnetoresistance in Mn ion-implanted GaAs:Zn nanowires. Applied Physics Letters, 2014, 104, 153112.	1.5	8
117	Polarization features of optically pumped CdS nanowire lasers. Journal Physics D: Applied Physics, 2014, 47, 394012.	1.3	23
118	Temperature and bias-voltage dependence of atomic-layer-deposited HfO2-based magnetic tunnel junctions. Applied Physics Letters, 2014, 105, .	1.5	8
119	Phonon-assisted lasing in ZnO microwires at room temperature. Applied Physics Letters, 2014, 105, .	1.5	12
120	Nano-X-ray diffraction study of single Co-implanted ZnO nanowires. Physica Status Solidi (A) Applications and Materials Science, 2014, 211, 2523-2526.	0.8	4
121	Functional ZnO/polymer core-shell nanowires fabricated by oxidative chemical vapour deposition. Journal Physics D: Applied Physics, 2014, 47, 394004.	1.3	11
122	Enhanced sputtering and incorporation of Mn in implanted GaAs and ZnO nanowires. Journal Physics D: Applied Physics, 2014, 47, 394003.	1.3	24
123	Flash Sintering of Nanocrystalline Zinc Oxide and its Influence on Microstructure and Defect Formation. Journal of the American Ceramic Society, 2014, 97, 1728-1735.	1.9	131
124	Defect studies on Ar-implanted ZnO thin films. Physica Status Solidi (B): Basic Research, 2014, 251, 937-941.	0.7	1
125	High lateral resolution energy dispersive X-ray spectroscopy and cathodoluminescence on lamellae of CIGSe solar cells. , 2014, , .		1
126	Structural order in single Coâ€implanted ZnO nanowires. Physica Status Solidi (A) Applications and Materials Science, 2014, 211, 483-487.	0.8	4

#	Article	IF	CITATIONS
127	Amphoteric Nature of Sn in CdS Nanowires. Nano Letters, 2014, 14, 518-523.	4.5	32
128	Electron-beam-induced current at absorber back surfaces of Cu(In,Ga)Se2 thin-film solar cells. Journal of Applied Physics, 2014, 115, .	1.1	24
129	Local Ion Irradiation-Induced Resistive Threshold and Memory Switching in Nb ₂ O ₅ /NbO _{<i>x</i>} Films. ACS Applied Materials & Interfaces, 2014, 6, 17474-17480.	4.0	50
130	Highly efficient visible-light driven photocatalysts: a case of zinc stannate based nanocrystal assemblies. Journal of Materials Chemistry A, 2014, 2, 4157-4167.	5.2	40
131	Hot-Electron Injection in Au Nanorod–ZnO Nanowire Hybrid Device for Near-Infrared Photodetection. Nano Letters, 2014, 14, 6202-6209.	4.5	141
132	Gate modulation of below-band-gap photoconductivity in ZnO nanowire field-effect-transistors. Journal Physics D: Applied Physics, 2014, 47, 394014.	1.3	6
133	Structural properties of zinc oxide deposited using atmospheric pressure combustion chemical vapour deposition. Thin Solid Films, 2014, 565, 45-53.	0.8	11
134	Single Step Integration of ZnO Nano- and Microneedles in Si Trenches by Novel Flame Transport Approach: Whispering Gallery Modes and Photocatalytic Properties. ACS Applied Materials & Interfaces, 2014, 6, 7806-7815.	4.0	156
135	Deep-level emission in ZnO nanowires and bulk crystals: Excitation-intensity dependence versus crystalline quality. Journal of Applied Physics, 2014, 115, 233516.	1.1	11
136	Improving the Optical Properties of Self-Catalyzed GaN Microrods toward Whispering Gallery Mode Lasing. ACS Photonics, 2014, 1, 990-997.	3.2	37
137	Ultrafast plasmonic nanowire lasers near the surface plasmon frequency. Nature Physics, 2014, 10, 870-876.	6.5	262
138	Intense Intrashell Luminescence of Eu-Doped Single ZnO Nanowires at Room Temperature by Implantation Created Eu–O _i Complexes. Nano Letters, 2014, 14, 4523-4528.	4.5	63
139	Utilizing dynamic annealing during ion implantation: synthesis of silver nanoparticles in crystalline lithium niobate. Nanotechnology, 2014, 25, 135611.	1.3	6
140	Ultrafast ZnO nanowire lasers: nanoplasmonic acceleration of gain dynamics at the surface plasmon polariton frequency. , 2014, , .		2
141	DNA hybridization assay at individual, biofunctionalized zinc oxide nanowires. Journal of Biophotonics, 2013, 6, 143-147.	1.1	8
142	Intense intraâ€3d luminescence and waveguide properties of single Coâ€doped ZnO nanowires. Physica Status Solidi - Rapid Research Letters, 2013, 7, 886-889.	1.2	9
143	The Physics of Copper Oxide (Cu2O). Semiconductors and Semimetals, 2013, , 201-226.	0.4	34
144	Continuous Wave Nanowire Lasing. Nano Letters, 2013, 13, 3602-3606.	4.5	52

#	Article	IF	CITATIONS
145	CdTe grown under Cd/Te excess at very low temperatures for solar cells. Journal of Applied Physics, 2013, 113, .	1.1	7
146	Magnetic Polarons and Large Negative Magnetoresistance in GaAs Nanowires Implanted with Mn Ions. Nano Letters, 2013, 13, 5079-5084.	4.5	26
147	Local lattice distortions in single Co-implanted ZnO nanowires. Applied Physics Letters, 2013, 103, 141911.	1.5	10
148	Room temperature plasmonic nanowire laser near the surface plasmon frequency. , 2013, , .		0
149	A General Approach toward Shape-Controlled Synthesis of Silicon Nanowires. Nano Letters, 2013, 13, 21-25.	4.5	4
150	Luminescent ordered arrays of nanoporous silicon nanopillars and silicon nanopillars with nanoporous shells. Materials Letters, 2013, 98, 186-189.	1.3	8
151	Buffer-free Cu(In,Ga)Se2-solar cells by near-surface ion implantation. Solar Energy Materials and Solar Cells, 2013, 116, 43-48.	3.0	7
152	Controlled synthesis of ultrathin ZnO nanowires using micellar gold nanoparticles as catalyst templates. Nanoscale, 2013, 5, 7046.	2.8	15
153	Spatially resolved measurements of charge carrier lifetimes in CdTe solar cells. Journal of Applied Physics, 2013, 113, .	1.1	14
154	Luminescence and energy transfer processes in ensembles and single Mn or Tb doped ZnS nanowires. Journal of Applied Physics, 2013, 113, 073506.	1.1	5
155	Ordered arrays of patterned nanoporous silicon. Journal of Micromechanics and Microengineering, 2013, 23, 074004.	1.5	6
156	A CEMS search for precipitate formation in 57Fe implanted ZnO. , 2013, , 485-488.		0
157	Modal gain and its diameter dependence in single-ZnO micro- and nanowires. Semiconductor Science and Technology, 2012, 27, 015005.	1.0	9
158	Extension of the cubic boron nitride thin film growth phase diagram. Diamond and Related Materials, 2012, 22, 88-91.	1.8	4
159	Low threshold room-temperature lasing of CdS nanowires. Nanotechnology, 2012, 23, 365204.	1.3	48
160	Hexagonal boron nitride nanowalls: physical vapour deposition, 2D/3D morphology and spectroscopic analysis. Journal Physics D: Applied Physics, 2012, 45, 135302.	1.3	22
161	Protein Adsorption on Nano-scaled, Rippled TiO2and Si Surfaces. Biointerphases, 2012, 7, 55.	0.6	23
162	Maxwell-Wagner polarization in Cu(In,Ga)(S,Se) ₂ . Applied Physics Letters, 2012, 100, 252111.	1.5	15

#	Article	IF	CITATIONS
163	Hopping Conduction in Mn Ion-Implanted GaAs Nanowires. Nano Letters, 2012, 12, 4838-4842.	4.5	39
164	Correlation between damage evolution, cluster formation and optical properties of silver implanted lithium niobate. Nuclear Instruments & Methods in Physics Research B, 2012, 286, 67-71.	0.6	11
165	Direct Determination of Minority Carrier Diffusion Lengths at Axial GaAs Nanowire p–n Junctions. Nano Letters, 2012, 12, 1453-1458.	4.5	112
166	Thermoelectric Characterization of Electronic Properties of GaMnAs Nanowires. Journal of Nanotechnology, 2012, 2012, 1-5.	1.5	10
167	Quantification of impurity concentration in Cu ₂ O and CuO via secondary ion mass spectrometry. Physica Status Solidi (B): Basic Research, 2012, 249, 801-811.	0.7	8
168	Binary copper oxide semiconductors: From materials towards devices. Physica Status Solidi (B): Basic Research, 2012, 249, 1487-1509.	0.7	547
169	A CEMS search for precipitate formation in 57Fe implanted ZnO. Hyperfine Interactions, 2012, 207, 49-52.	0.2	3
170	Significant stress reduction of cBN layers upon ion irradiation at elevated temperatures. Nuclear Instruments & Methods in Physics Research B, 2012, 280, 18-21.	0.6	0
171	Luminescence properties of Ga-graded Cu(In,Ga)Se2 thin films. Thin Solid Films, 2012, 520, 3657-3662.	0.8	5
172	Composition and texture of barium silicate crystals in fresnoite glass-ceramics by various scanning electron microscopic techniques. CrystEngComm, 2011, 13, 3383.	1.3	14
173	Strongly Enhanced Molecular Fluorescence inside a Nanoscale Waveguide Gap. Nano Letters, 2011, 11, 4907-4911.	4.5	94
174	Permanent bending and alignment of ZnO nanowires. Nanotechnology, 2011, 22, 185307.	1.3	64
175	A New Route toward Semiconductor Nanospintronics: Highly Mn-Doped GaAs Nanowires Realized by Ion-Implantation under Dynamic Annealing Conditions. Nano Letters, 2011, 11, 3935-3940.	4.5	47
176	Nano-X-ray Absorption Spectroscopy of Single Co-Implanted ZnO Nanowires. Nano Letters, 2011, 11, 5322-5326.	4.5	67
177	Near-interface doping by ion implantation in Cu(In,Ga)Se2 solar cells. Thin Solid Films, 2011, 519, 7276-7279.	0.8	1
178	Ion beam irradiation of nanostructures – A 3D Monte Carlo simulation code. Nuclear Instruments & Methods in Physics Research B, 2011, 269, 2133-2138.	0.6	97
179	Biofunctionalization of zinc oxide nanowires for DNA sensory applications. Nanoscale Research Letters, 2011, 6, 511.	3.1	36
180	Synchrotron fluorescence nanoimaging of a single Coâ€implanted ZnO nanowire. Physica Status Solidi - Rapid Research Letters, 2011, 5, 283-285.	1.2	11

#	Article	IF	CITATIONS
181	Temperature-dependent photoconductance of heavily doped ZnO nanowires. Nano Research, 2011, 4, 1110-1116.	5.8	14
182	Defect induced changes on the excitation transfer dynamics in ZnS/Mn nanowires. Nanoscale Research Letters, 2011, 6, 228.	3.1	5
183	Increased homogeneity and open-circuit voltage of Cu(In,Ca)Se2 solar cells due to higher deposition temperature. Solar Energy Materials and Solar Cells, 2011, 95, 1028-1030.	3.0	39
184	Magnetoelectronic properties of Gd-implanted tetrahedral amorphous carbon. Physical Review B, 2011, 84, .	1.1	8
185	Determination of secondary ion mass spectrometry relative sensitivity factors for polar and non-polar ZnO. Journal of Applied Physics, 2011, 110, .	1.1	6
186	Persistent ion beam induced conductivity in zinc oxide nanowires. Applied Physics Letters, 2011, 99, 252105.	1.5	13
187	Coupling Molecular Photoluminescence Into Deep Sub-Wavelength Plasmon Waveguides. , 2011, , .		0
188	Bimodal range distributions of low-energy carbon ions in tetrahedral amorphous carbon. Europhysics Letters, 2010, 90, 46002.	0.7	2
189	Phase diagram of Si nanowire growth by disproportionation of SiO. Journal of Crystal Growth, 2010, 312, 1751-1754.	0.7	7
190	Self-organized nanostructuring of composite coatings at high temperatures for drag reduction and self-cleaning. Surface and Coatings Technology, 2010, 205, 1584-1588.	2.2	1
191	Ion beam doping of semiconductor nanowires. Materials Science and Engineering Reports, 2010, 70, 30-43.	14.8	96
192	Annealing effects and generation of secondary phases in ZnO after highâ€dose transition metal implantation. Physica Status Solidi (B): Basic Research, 2010, 247, 1469-1471.	0.7	5
193	Optical and magnetic properties of quasi oneâ€dimensional dilute magnetic ZnMnS and antiferromagnetic MnS. Physica Status Solidi (B): Basic Research, 2010, 247, 2522-2536.	0.7	7
194	Tailoring the properties of semiconductor nanowires using ion beams. Physica Status Solidi (B): Basic Research, 2010, 247, 2329-2337.	0.7	18
195	Stable enhancement of near-band-edge emission of ZnO nanowires by hydrogen incorporation. Nanotechnology, 2010, 21, 065709.	1.3	60
196	Hopping Conduction Observed in Thermal Admittance Spectroscopy. Physical Review Letters, 2010, 104, 226403.	2.9	43
197	Epitactically Interpenetrated High Quality ZnO Nanostructured Junctions on Microchips Grown by the Vaporâ^'Liquidâ^'Solid Method. Crystal Growth and Design, 2010, 10, 2842-2846.	1.4	62
198	Optically pumped nanowire lasers: invited review. Semiconductor Science and Technology, 2010, 25, 024001.	1.0	171

#	Article	IF	CITATIONS
199	Ion beam doping of semiconductor nanowires. , 2010, , .		0
200	Structure and defects of epitaxial Si(111) layers on Y[sub 2]O[sub 3](111)/Si(111) support systems. Journal of Vacuum Science & Technology B, 2009, 27, 305.	1.3	11
201	Self-organized formation of layered carbon–copper nanocomposite films by ion deposition. Nuclear Instruments & Methods in Physics Research B, 2009, 267, 1356-1359.	0.6	4
202	Alignment of Semiconductor Nanowires Using Ion Beams. Small, 2009, 5, 2576-2580.	5.2	66
203	Evidence of intrinsic ferromagnetism in individual dilute magnetic semiconducting nanostructures. Nature Nanotechnology, 2009, 4, 523-527.	15.6	149
204	Simulation and fitting of high resolution Rutherford backscattering spectra. Nuclear Instruments & Methods in Physics Research B, 2009, 267, 1737-1739.	0.6	5
205	Morphology of Si surfaces sputter-eroded by low-energy Xe-ions at glancing incident angle. Surface and Coatings Technology, 2009, 203, 2395-2398.	2.2	13
206	Influence of metallic coatings on the photoluminescence properties of ZnO nanowires. Physica Status Solidi - Rapid Research Letters, 2009, 3, 166-168.	1.2	16
207	Axial p-n Junctions Realized in Silicon Nanowires by Ion Implantation. Nano Letters, 2009, 9, 1341-1344.	4.5	107
208	A Search for Magnetic Effects in Ion Implanted ZnO and SiC. , 2009, , .		0
209	Intra-shell luminescence of transition-metal-implanted zinc oxide nanowires. Nanotechnology, 2009, 20, 135704.	1.3	45
210	The influence of local heating by nonlinear pulsed laser excitation on the transmission characteristics of a ZnO nanowire waveguide. Nanotechnology, 2009, 20, 095702.	1.3	7
211	Secondary phase segregation in heavily transition metal implanted ZnO. Journal of Applied Physics, 2009, 105, .	1.1	49
212	Exciton-related electroluminescence from ZnO nanowire light-emitting diodes. Applied Physics Letters, 2009, 94, .	1.5	90
213	Electric field gradients at 151Eu sites in GaN. Hyperfine Interactions, 2008, 184, 213-216.	0.2	0
214	Nanomaterial electronic structure investigation by valence electron energy loss spectroscopy—An example of doped ZnO nanowires. Micron, 2008, 39, 703-708.	1.1	5
215	Laser action in nanowires: Observation of the transition from amplified spontaneous emission to laser oscillation. Applied Physics Letters, 2008, 93, 051101.	1.5	223
216	Intense white photoluminescence emission of V-implanted zinc oxide thin films. Journal of Applied Physics, 2008, 104, .	1.1	25

#	Article	IF	CITATIONS
217	Structural impact of Mn implantation on ZnO. New Journal of Physics, 2008, 10, 043004.	1.2	61
218	Ion Beam Doping of Silicon Nanowires. Nano Letters, 2008, 8, 2188-2193.	4.5	83
219	Comparative study of self-assembling of multilayers using reactive sputter deposition and mass selective ion beam deposition. Diamond and Related Materials, 2008, 17, 1494-1497.	1.8	6
220	Scalable Fabrication of Nanowire Photonic and Electronic Circuits Using Spin-on Glass. Nano Letters, 2008, 8, 1695-1699.	4.5	82
221	Rare Earth Doped Zinc Oxide Nanowires. Journal of Nanoscience and Nanotechnology, 2008, 8, 244-251.	0.9	33
222	P-type doping of GaAs nanowires. Applied Physics Letters, 2008, 92, 163107.	1.5	39
223	Characterization of the donor-acceptor-pair transition in Nitrogen-implanted zinc oxide. Journal of Applied Physics, 2008, 103, 083513.	1.1	10
224	Energy Transfer and Dynamics of the Mn 3d5 Luminescence in Low Dimensional (Zn,Mn)S Nanostructures. Journal of the Korean Physical Society, 2008, 53, 2830-2834.	0.3	2
225	Ultrafast carrier dynamics in tetrahedral amorphous carbon: carrier trapping versus electron–hole recombination. New Journal of Physics, 2007, 9, 404-404.	1.2	11
226	Ion induced nanoscale surface ripples on ferromagnetic films with correlated magnetic texture. New Journal of Physics, 2007, 9, 29-29.	1.2	39
227	Properties of V-implanted ZnO nanorods. Nanotechnology, 2007, 18, 125609.	1.3	6
228	Dimensional dependence of the dynamics of the <mml:math xmlns:mml="http://www.w3.org/1998/Math/MathML" display="inline"><mml:mrow><mml:mi mathvariant="normal">Mn<mml:mspace <br="" width="0.2em">/><mml:mn>3</mml:mn><mml:msup><mml:mi>d</mml:mi><mml:mn>5</mml:mn></mml:msup></mml:mspace></mml:mi </mml:mrow></mml:math 	1.1 <td>13 th>luminesce</td>	13 th>luminesce
229	in (Zn, Mn)S nanowires and nanobelts. Physical Review B, 2007, 76, . Unambiguous identification of the PL-19 line in zinc oxide. Applied Physics Letters, 2007, 90, 012107.	1.5	38
230	Modeling the Carrier Mobility in Nanowire Channel FET. Materials Research Society Symposia Proceedings, 2007, 1017, 139.	0.1	4
231	Finite size effect in ZnO nanowires. Applied Physics Letters, 2007, 90, 113101.	1.5	115
232	Optical size effects in ultrathin ZnO nanowires. Nanotechnology, 2007, 18, 435701.	1.3	57
233	High-Order Waveguide Modes in ZnO Nanowires. Nano Letters, 2007, 7, 3675-3680.	4.5	149
234	Magnetic characterization of ZnO doped with vanadium. Superlattices and Microstructures, 2007, 42, 236-241.	1.4	18

#	Article	IF	CITATIONS
235	Sputter erosion of ferromagnetic thin films. Surface and Coatings Technology, 2007, 201, 8477-8481.	2.2	5
236	Pattern formation of Si surfaces by low-energy sputter erosion. Surface and Coatings Technology, 2007, 201, 8299-8302.	2.2	16
237	Morphological change of carbon surfaces by sputter erosion. Nuclear Instruments & Methods in Physics Research B, 2007, 256, 378-382.	0.6	20
238	High-performance ZnO nanowire field effect transistors. Applied Physics Letters, 2006, 89, 133113.	1.5	223
239	The effect of substrate surface roughness on the nucleation of cubic boron nitride films. Diamond and Related Materials, 2006, 15, 55-60.	1.8	16
240	Luminescence centres in silica nanowires. Nanotechnology, 2006, 17, 3215-3218.	1.3	41
241	Catalystâ^'Nanostructure Interaction in the Growth of 1-D ZnO Nanostructures. Journal of Physical Chemistry B, 2006, 110, 1656-1660.	1.2	101
242	Self-assembled nano-scale multilayer formation using physical vapor deposition methods. Nuclear Instruments & Methods in Physics Research B, 2006, 242, 261-264.	0.6	9
243	Catalyst–nanostructure interaction and growth of ZnS nanobelts. Nanotechnology, 2006, 17, 1067-1071.	1.3	27
244	Magnetic Rare Earth (Gd) Implanted Tetrahedral Amorphous Carbon (ta-C). Materials Research Society Symposia Proceedings, 2006, 941, 1.	0.1	2
245	Optical activation of implanted impurities in ZnS nanowires. Journal of Vacuum Science and Technology A: Vacuum, Surfaces and Films, 2006, 24, 1356-1359.	0.9	5
246	Growth and Properties of Zincsulfide Nanowires. NATO Science Series Series II, Mathematics, Physics and Chemistry, 2006, , 407-410.	0.1	2
247	Cubic boron nitride thin film growth by boron and nitrogen ion implantation. Physical Review B, 2005, 72, .	1.1	9
248	Nucleation mechanism of the seed of tetrapod ZnO nanostructures. Journal of Applied Physics, 2005, 98, 034307.	1.1	82
249	Self-organized nanoscale multilayer growth in hyperthermal ion deposition. Physical Review B, 2004, 70, .	1.1	32
250	The role of ion energy on the growth mechanism of cubic boron nitride films. Thin Solid Films, 2004, 447-448, 125-130.	0.8	7
251	Wurtzite ZnS nanosaws produced by polar surfaces. Chemical Physics Letters, 2004, 385, 8-11.	1.2	123
252	Field emission studies on swift heavy ion irradiated tetrahedral amorphous carbon. Diamond and Related Materials, 2004, 13, 1032-1036.	1.8	10

#	Article	IF	CITATIONS
253	Manganese-doped ZnO nanobelts for spintronics. Applied Physics Letters, 2004, 84, 783-785.	1.5	301
254	On the mechanisms of cubic boron nitride film growth. Diamond and Related Materials, 2004, 13, 1103-1110.	1.8	30
255	Ion-beam synthesis and growth mechanism of diamond-like materials. Applied Physics A: Materials Science and Processing, 2003, 77, 39-50.	1.1	26
256	Electron emission channeling spectroscopy using X-ray CCD detectors. Nuclear Instruments and Methods in Physics Research, Section A: Accelerators, Spectrometers, Detectors and Associated Equipment, 2003, 512, 378-385.	0.7	6
257	Europium doping of c-BN and ta-C thin films. Diamond and Related Materials, 2003, 12, 1182-1185.	1.8	15
258	Conductivity of ion tracks in diamond-like carbon films. Diamond and Related Materials, 2003, 12, 938-941.	1.8	19
259	Phase formation of boron nitride thin films under the influence of impurity atoms. Diamond and Related Materials, 2003, 12, 1173-1177.	1.8	6
260	Ion energy thresholds and stability of cubic boron nitride. Diamond and Related Materials, 2003, 12, 1877-1882.	1.8	12
261	Diffusion in diamond-like carbon. Diamond and Related Materials, 2003, 12, 2042-2050.	1.8	21
262	Ion beam synthesis of diamond-like carbon thin films containing copper nanocrystals. Journal of Applied Physics, 2003, 93, 1203-1207.	1.1	29
263	Fundamental role of ion bombardment for the synthesis of cubic boron nitride films. Physical Review B, 2002, 65, .	1.1	28
264	Surface Brillouin scattering of cubic boron nitride films. Journal of Applied Physics, 2002, 91, 4196-4204.	1.1	19
265	Comment on "On the mechanism of the cubic phase formation in the boron nitride thin-film systems― [Appl. Phys. Lett. 79, 353 (2001)]. Applied Physics Letters, 2002, 80, 1306-1307.	1.5	1
266	Lattice Location and Cathodoluminescence Studies of Ytterbium/Thulium Implanted 2H-Aluminium Nitride. Materials Research Society Symposia Proceedings, 2002, 743, L6.16.1.	0.1	7
267	Lanthanide Doped Cubic Boron Nitride. Materials Research Society Symposia Proceedings, 2002, 744, 1.	0.1	3
268	<title>Elastic properties of cBN films by surface Brillouin scattering</title> . , 2002, , .		2
269	Lattice site location of ion-implanted 8Li in Silicon Carbide. Journal of Applied Physics, 2002, 91, 1046-1052.	1.1	11
270	Implantation sites of Ce and Gd in diamond. Nuclear Instruments & Methods in Physics Research B, 2002, 190, 835-839.	0.6	8

#	Article	IF	CITATIONS
271	Ion beam synthesis of boron carbide thin films. Surface and Coatings Technology, 2002, 158-159, 382-387.	2.2	68
272	Ion beam synthesis of amorphous carbon thin films containing metallic nanoclusters. Surface and Coatings Technology, 2002, 158-159, 114-119.	2.2	25
273	Graphitic nanowires embedded in diamond-like carbon films. AIP Conference Proceedings, 2001, , .	0.3	3
274	Ion implantation into gallium nitride. Physics Reports, 2001, 351, 349-385.	10.3	127
275	Conventional and pendeo-epitaxial growth of GaN(0001) thin films on Si(111) substrates. Journal of Crystal Growth, 2001, 231, 335-341.	0.7	35
276	Film growth using mass-separated ion beams. AIP Conference Proceedings, 2001, , .	0.3	6
277	High-resolution elastic recoil detection utilizing Bayesian probability theory. Nuclear Instruments & Methods in Physics Research B, 2001, 183, 48-61.	0.6	20
278	Ion beam deposition of fluorinated amorphous carbon. Journal of Applied Physics, 2001, 90, 4237-4245.	1.1	25
279	Implantation sites of In, Cd, and Hf ions in diamond. Physical Review B, 2001, 64, .	1.1	8
280	Cubic boron nitride thin film heteroepitaxy. Journal of Applied Physics, 2001, 90, 3248-3254.	1.1	33
281	Superhard, conductive coatings for atomic force microscopy cantilevers. Applied Physics Letters, 2001, 79, 3053-3055.	1.5	5
282	Ion beam erosion of graphite surfaces studied by STM: Ripples, self-affine roughening and near-surface damage accumulation. Nuclear Instruments & Methods in Physics Research B, 2000, 161-163, 958-962.	0.6	20
283	Pendeo-epitaxial growth of gallium nitride on silicon substrates. Journal of Electronic Materials, 2000, 29, 306-310.	1.0	21
284	Photoluminescence characterization of Mg implanted GaN. MRS Internet Journal of Nitride Semiconductor Research, 2000, 5, 725-732.	1.0	1
285	Hydrogen-plasma etching of ion beam deposited c-BN films: An in situ investigation of the surface with electron spectroscopy. Journal of Applied Physics, 2000, 88, 5597-5604.	1.1	20
286	Ion implanted dopants in GaN and AlN: Lattice sites, annealing behavior, and defect recovery. Journal of Applied Physics, 2000, 87, 2149-2157.	1.1	52
287	Growth, doping and applications of cubic boron nitride thin films. Diamond and Related Materials, 2000, 9, 1767-1773.	1.8	24
288	Characterization of Be-Implanted GaN Annealed at High Temperatures. MRS Internet Journal of Nitride Semiconductor Research, 1999, 4, 203-208.	1.0	1

#	Article	IF	CITATIONS
289	Elastic properties of hard cBN films by surface Brillouin scattering. , 1999, , .		1
290	Lattice site and diffusion of ion-implanted Li in as-grown and Se-rich ZnSe. Physica B: Condensed Matter, 1999, 273-274, 875-878.	1.3	3
291	Electrically conducting ion tracks in diamond-like carbon films for field emission. Applied Physics A: Materials Science and Processing, 1999, 69, 239-240.	1.1	42
292	Valence band discontinuity of the (0001) 2H-GaN / (111) 3C-SiC interface. Journal of Electronic Materials, 1999, 28, L34-L37.	1.0	25
293	Valence band discontinuity, surface reconstruction, and chemistry of (0001), (0001̄), and (11̄00) 2H–AlN/6H–SiC interfaces. Journal of Applied Physics, 1999, 86, 4483-4490.	1.1	34
294	Ion implantation and annealing of diamond studied by emission channeling and cathodoluminescence. Diamond and Related Materials, 1999, 8, 1623-1630.	1.8	23
295	Room temperature growth of cubic boron nitride. Applied Physics Letters, 1999, 74, 1552-1554.	1.5	51
296	Pendeo-Epitaxial Growth of GaN on SiC and Silicon Substrates via Metalorganic Chemical Vapor Deposition. Materials Research Society Symposia Proceedings, 1999, 572, 307.	0.1	2
297	Properties of Ion Beam Deposited Tetrahedral Fluorinated Amorphous Carbon Films (ta-C:F). Materials Research Society Symposia Proceedings, 1999, 593, 335.	0.1	0
298	Photoluminescence characterization of Mg implanted GaN. Materials Research Society Symposia Proceedings, 1999, 595, 1.	0.1	0
299	Cylindrical spike model for the formation of diamondlike thin films by ion deposition. Applied Physics A: Materials Science and Processing, 1998, 66, 153-181.	1.1	154
300	Carbon transport in Si(001) and nucleation of diamond-like carbon layers during mass selected carbon ion beam deposition. Diamond and Related Materials, 1998, 7, 15-22.	1.8	8
301	Structural and electronic properties of boron nitride thin films containing silicon. Journal of Applied Physics, 1998, 84, 5046-5051.	1.1	52
302	Cleaning of AlN and GaN surfaces. Journal of Applied Physics, 1998, 84, 5248-5260.	1.1	277
303	Carbon nitride deposited using energetic species: A review on XPS studies. Physical Review B, 1998, 58, 2207-2215.	1.1	394
304	Optical activation of Be implanted into GaN. Applied Physics Letters, 1998, 73, 1622-1624.	1.5	61
305	X-ray photoelectron diffraction from (3×3) and (â^š3×â^š3)R 30° (0001)Si 6H–SiC surfaces. Journal of Applied Physics, 1998, 84, 6042-6048.	1.1	25
306	Dependence of (0001) GaN/AlN valence band discontinuity on growth temperature and surface reconstruction. Journal of Applied Physics, 1998, 84, 2086-2090.	1.1	77

#	Article	IF	CITATIONS
307	Lattice site location studies of ion implanted 8Li in GaN. Journal of Applied Physics, 1998, 84, 3085-3089.	1.1	16
308	Characterization of Be-Implanted GaN Annealed at High Temperatures. Materials Research Society Symposia Proceedings, 1998, 537, 1.	0.1	1
309	Thresholds for the phase formation of cubic boron nitride thin films. Physical Review B, 1997, 55, 13230-13233.	1.1	92
310	Substitutional phosphorus doping of diamond by ion implantation. Journal of Applied Physics, 1997, 81, 2566-2569.	1.1	26
311	Observation of boron bound excitons in boron-implanted and annealed natural IIa diamonds. Applied Physics Letters, 1997, 71, 2668-2670.	1.5	25
312	Modeling of the Ion-Beam Growth of Covalently-Bonded Diamondlike Materials. Materials Research Society Symposia Proceedings, 1997, 498, 129.	0.1	3
313	Recovery of Structural Defects in GaN After Heavy Ion Implantation. Materials Research Society Symposia Proceedings, 1997, 468, 407.	0.1	25
314	Lattice Location and Luminescence Behavior of Rare Earth Elements Implanted in GaN. Materials Research Society Symposia Proceedings, 1997, 482, 1016.	0.1	17
315	Electrical properties and thermal stability of ion beam deposited BN thin films. Diamond and Related Materials, 1997, 6, 1129-1134.	1.8	56
316	Electronic and atomic structure of undoped and doped ta-C films. Diamond and Related Materials, 1997, 6, 830-834.	1.8	36
317	Amorphization of ZnSe by ion implantation at low temperatures. , 1996, , 907-911.		Ο
318	Quantitative Analysis of Chemically-Enhanced Sputtering during lon Beam Deposition of Carbon Nitride Thin Films. Materials Research Society Symposia Proceedings, 1996, 438, 575.	0.1	4
319	Behavior Of The Potential N-Type Dopants P And As In Diamondafter Low Dose Ion Implantation. Materials Research Society Symposia Proceedings, 1996, 442, 675.	0.1	2
320	Thin Film Growth of Group III Nitrides by Mass Separated Ion Beam Deposition. Materials Research Society Symposia Proceedings, 1996, 449, 331.	0.1	2
321	Emission channeling study of annealing of radiation damage in heavy-ion implanted diamond. Nuclear Instruments & Methods in Physics Research B, 1996, 118, 72-75.	0.6	28
322	Alpha-emission channeling investigations of the lattice location of Li in Ge. Nuclear Instruments & Methods in Physics Research B, 1996, 118, 76-81.	0.6	8
323	Lattice sites of Li in CdTe. Journal of Crystal Growth, 1996, 161, 168-171.	0.7	4
324	Thermal stability of substitutional Ag in CdTe. Journal of Crystal Growth, 1996, 161, 172-176.	0.7	8

#	Article	IF	CITATIONS
325	Lattice sites of Li in CdTe. , 1996, , 168-171.		0
326	Characterization of cubic boron nitride films grown by mass separated ion beam deposition. , 1996, , 153-158.		0
327	Modeling detector response for neutron depth profiling. Nuclear Instruments and Methods in Physics Research, Section A: Accelerators, Spectrometers, Detectors and Associated Equipment, 1995, 366, 137-144.	0.7	11
328	Characterization of cubic boron nitride films grown by mass separated ion beam deposition. Nuclear Instruments & Methods in Physics Research B, 1995, 106, 153-158.	0.6	40
329	Lattice sites of arsenic ions implanted in diamond. Journal of Applied Physics, 1995, 78, 5180-5182.	1.1	16
330	Lattice sites of ion implanted Li in diamond. Applied Physics Letters, 1995, 66, 2733-2735.	1.5	38
331	Conduction processes in boron- and nitrogen-doped diamond-like carbon films prepared by mass-separated ion beam deposition. Diamond and Related Materials, 1995, 4, 666-672.	1.8	105
332	Cubic boron nitride films grown by low energy B+ and N+ ion beam deposition. Applied Physics Letters, 1995, 67, 46-48.	1.5	92
333	Li on bond-center sites in Si. Physical Review B, 1994, 50, 2176-2180.	1.1	12
334	Lattice sites of ion implanted Li in indium antimonide. Nuclear Instruments & Methods in Physics Research B, 1994, 85, 468-473.	0.6	13
335	Study of Indium Implanted GaAs: Positron Annihilation and Electrical Measurements. Materials Science Forum 1993 143-147 305-310	0.3	0